# Modelling compressive basic creep of concrete at early age

Brice Delsaute, Jean Michel Torrenti, Boumediene Nedjar, Stéphanie Staquet, Agathe Bourchy, Matthieu Briffaut

# Modelling compressive basic creep of concrete at early age

Brice Delsaute[a], Jean Michel Torrenti[b,c,*], Boumediene Nedjar[d], Stéphanie Staquet[a], Agathe Bourchy[b], Matthieu Briffaut[e]

[a] *BATir department, Université libre de Bruxelles, Belgium*
[b] *Département Matériaux et Structures - Mast, Université Gustave Eiffel, Champs-sur-Marne, France*
[c] *ESITC-Paris, France*
[d] *Université d'Evry Paris-Saclay, LMEE, 91020, Evry, France*
[e] *Laboratoire de Mécanique, Multiphysique, Multiéchelle (LaMcube), Ecole Centrale Lille, France*

* Corresponding author. Tel.: +33 6 89 12 28 50
E-mail address: jean-michel.torrenti@univ-eiffel.fr

**ABSTRACT**

Basic creep plays an important role for assessing the risk of early age cracking in massive structures. In recent decades, several models have been developed to characterize how the hydration process impacts the development of basic creep. This study investigates the basic creep of various concrete mixes across different ages at loading. The focus of analysis includes the very early stages (less than 24 hours) and early stages (less than 28 days) of concrete development. It is shown that a logarithmic expression which contains two parameters describing the material can accurately model basic creep from a very early age. One parameter relates to the amplitude of creep and depends solely on the composition of the concrete. The other relates to the kinetics of creep and depends on the age of the material at loading and the nature of the concrete mixture. The logarithmic expression corresponds to a rheological model consisting of a single dashpot wherein viscosity exhibits a linear evolution over time. The model offers the advantage of eliminating the need to store the entire stress history for computing the stress resulting from the restriction of the free deformation. This approach significantly reduces computation time. Additionally, a power-law correlation is observed between the material ageing parameter and the degree of hydration. This relationship depends on the composition. At least two compressive creep tests performed at two different degrees of hydration are needed to calibrate the material parameters and consider the effect of ageing on basic creep compliance.

**Keywords:**

Concrete, creep, early age, rheological models

## 1. Introduction

To accurately assess the risk of early age cracking in concrete, it is of the utmost importance to accurately model temperature changes, the progress of the hydration reaction (via the degree of hydration, for instance) and the development of mechanical properties such as Young's modulus, Poisson's ratio, shrinkage and creep (Benboudjema and Torrenti 2008), (Benboudjema, Carette et al. 2019), (Wyrzykowski, Scrivener et al. 2019), (Fairbairn and Azenha 2019), (Azenha, Kanavaris et al. 2021). At an early age, the development of free deformation is subject to partial or complete restraint, resulting in the emergence of internal stresses. This restraint can manifest internally or externally. In the context of massive structures, internal restraint arises due to temperature gradients between the surface and the core of the concrete element. Specifically, post-setting temperature increases restrain thermal swelling in the core while inducing additional swelling at the surface. This leads to tensile stresses at the surface and compressive stresses in the core, defined by considering the viscoelastic behaviour of concrete through the elastic modulus and creep compliance. Creep strains play a crucial role in mitigating the development of these stresses. Conversely, when a concrete element experiences external restraint (e.g., connection between a new slab and existing beams), the heating phase generates compressive stresses followed by tensile stresses during the subsequent cooling period. In this scenario, creep strains continue to mitigate the stresses, but the occurrence of tensile stresses is expedited, happening earlier when the tensile strength is lower. This acceleration in tensile stress may potentially heighten the risk of cracking (refer to Figure 1) (Delsaute and Staquet 2020). It appears that creep can have a dual role, both positive and negative, in predicting the risk of cracking at an early age. Therefore, it becomes imperative to incorporate creep considerations into the modelling process to provide a comprehensive understanding of the concrete's behavior during this critical phase.

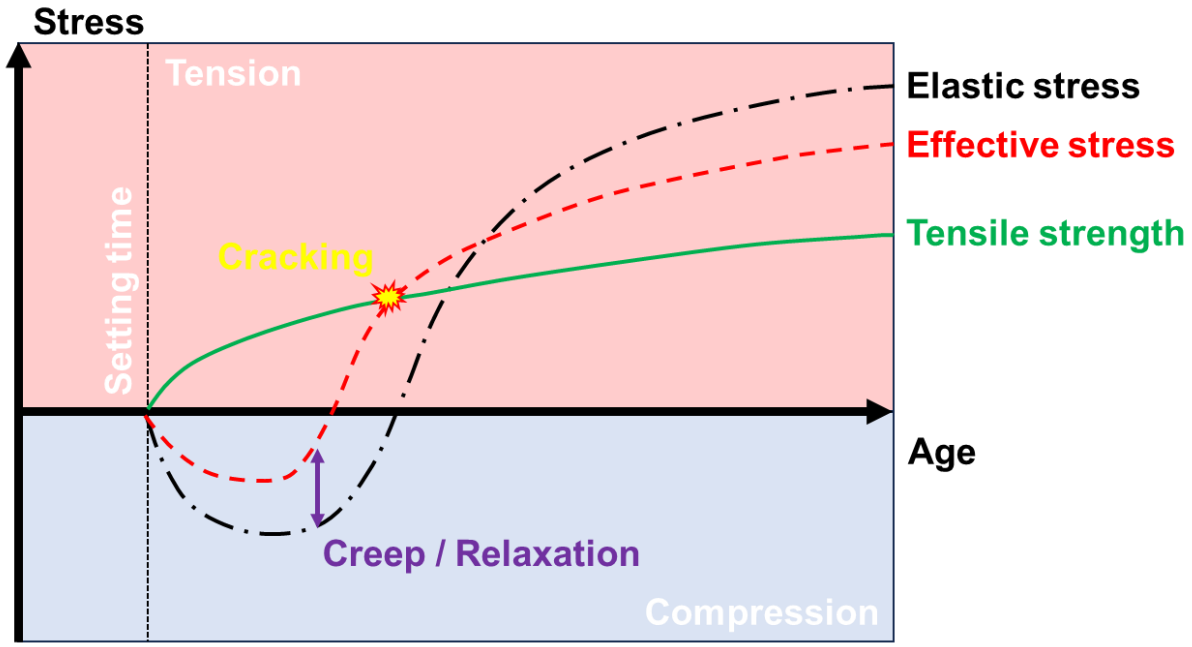


Figure 1 – Changes in stresses at early age in the case of restrained boundary conditions (Delsaute and Staquet 2020).

Because, in general, massive structures undergo major temporal and spatial variations in temperature at early age, drying creep is neglected in concrete as moisture diffusion is slow and the modelling is essentially concerned with basic creep (Cervera, Oliver et al. 1999), (Lackner and Mang 2004), (Gawin, Pesavento et al. 2006), (Benboudjema and Torrenti 2008), (Hilaire, Benboudjema et al. 2014), (Klemczak and Knoppik-Wróbel 2015), (Benboudjema, Carette et al. 2019), (Lacarriere, Sellier et al. 2020), (Binder, Königsberger et al. 2023) and (Ghasabeh and Göktepe 2023). In this paper, only compressive basic creep is considered. However, in a structure, as shown in Figure 1, compressive and tensile stresses should be considered when assessing the risks of cracking. Consequently, this work assumes that tensile creep strains are the opposite of compressive creep strains for a given level of stress. However, such a hypothesis is still debated (Briffaut, Benboudjema et al. 2012), (Rossi, Tailhan et al. 2013), (Ranaivomanana, Multon et al. 2013), (Klausen, Kanstad et al. 2017), (Khan, Castel et al. 2017), (Dabarera, Li et al. 2021).

Numerous researchers have experimentally investigated basic creep at early ages (Gutsch 2000), (Atrushi 2003), (De Schutter 1999), (Østergaard, Lange et al. 2001), (Briffaut, Benboudjema et al. 2012), (Wyrzykowski, Scrivener et al. 2019). In each instance, the analysis of basic creep compliance aging involves subjecting various samples to sustained loads lasting weeks or months at different ages. These investigations

have led to the development of different models addressing the aging of creep compliance. These models vary in their mathematical expressions, such as hyperbolic, logarithmic, or power, and the variables employed, such as time, equivalent time, and degree of hydration. Based on the findings, several theories have emerged in the literature, aiming to elucidate the physical origins of basic creep (Hilaire, Benboudjema et al. 2014), (Jiang, Yang et al. 2014), (Delsaute, Torrenti et al. 2017), (Wyrzykowski, Scrivener et al. 2019), (Dabarera, Li et al. 2021), (Su, Jia et al. 2023), (Binder, Königsberger et al. 2023). As explained in (Delsaute, Torrenti et al. 2017), the mechanisms presented in the literature can be divided into two categories : direct and indirect mechanisms. Direct mechanisms are related to the cement paste (water mobility, solidification, sliding of the C-S-H…) and can be divided in short- and long-term phenomena. Indirect mechanisms are related to micro-cracks formation in the cement paste or at the interface transition zone between the cement paste and the aggregate. Bažant et al. (Bazant, Hauggaard et al. 1997) explained it with the microprestress theory. In this theory, it is postulated that the origin of the creep is the shear slip at overstressed creep sites. As a result of a progressive relaxation of microprestress at the creep sites and consecutive increase of their apparent viscosity, the creep rate observed under constant applied stress declines over time. Bazant has modelled this behaviour by a non-asymptotic relation where a term is logarithmic.

Ulm et al. (Ulm, Le Maou et al. 1999), using Le Roy's tests (Leroy, Le Maou et al. 2017) have shown that the rate of basic creep compliance $J_{bc}^{*}$- i.e. the basic compliance $J_{bc}$ without the elastic part - has a linear evolution with time on a logarithmic scale. In this case, the basic creep compliance $J_{bc}^{*}(t, t_0)$ could be expressed, whatever the age at loading $t_0$, using a logarithmic function of time after loading, $t - t_0$ (Eq. 1):

$$J_{bc}^{*}(t, t_0) = \frac{1}{C} \cdot \ln\left(1 + \frac{t - t_0}{\tau(t_0)}\right) \quad (1)$$

This equation corresponds to the response of a dashpot with a viscosity that evolves linearly with time (this is highlighted later in Equation 3 and 4). There are now several experimental pieces of evidence that the basic creep compliance $J_{bc}^{*}(t, t_0)$ could be expressed with this equation. This behaviour has been observed at a macroscopic scale (see (Hanson 1953), (Larson and Jonasson 2003), (Muller, Anders et al. 2013), (Leroy, Le Maou et al. 2017) or (Torrenti 2018) and at a lower scale using micro-indentation (see (Vandamme and Ulm 2013), (Zhang, Le Roy et al. 2014), (Frech-Baronet, Sorelli et al. 2017), (Suwanmaneechot, Aili et al. 2020) or (Liu, Wei et al. 2022). It was introduced in the *fib* Model Code 2010 (Walraven and Bigaj-van Vliet 2013) and is now adopted for the next-generation Eurocode 2 (CEN 2023). Delsaute et al. have also demonstrated that

this equation may be used successfully at early age for both conventional concrete (Delsaute, Torrenti et al. 2017) and concrete containing recycled concrete aggregates (Delsaute and Staquet 2019).

However, in the initial stages of loading, additional phenomena may influence creep development, deviating from a logarithmic trend as reported in previous studies (Irfan-ul-Hassan, Königsberger et al. 2017), (Irfan-ul-Hassan, Pichler et al. 2016); (Delsaute, Torrenti et al. 2017). As demonstrated in (Delsaute, Torrenti et al. 2017), the basic creep compliance can be delineated into three components: (1) an initial short-term term characterized by a logarithmic expression, (2) a solidification term modelled using Kelvin-Voigt chains, and (3) a long-term described by a power expression. However, the model's complexity requires the knowledge of additional properties such as the evolution of the elastic modulus since setting and making it challenging for implementation in finite element analysis. Additionally, as discussed in (Mohammad, Rahimi-Aghdam et al. 2018), creep strain begins developing from the onset of load application and should be considered from that moment. However, for practical reasons, creep strains are typically set to zero upon reaching the target load. Consequently, the initial development of creep compliance or creep coefficient lacks well-defined experimental characterization. To address this issue, Bazant's team (Mohammad, Rahimi-Aghdam et al. 2018) proposed a methodology that involves fitting the initial data to a power law, where the exponent is a function of the loading duration and varies mainly between 0.10 and 0.35. Irfan et al. (Irfan-ul-Hassan, Königsberger et al. 2017), and subsequently Ali et al. (Naqi, Delsaute et al. 2023), demonstrated that it is feasible to model short-duration loading (5 minutes) by incorporating creep strains occurring during loading using a power law. The exponent for this model varies between 0.2 and 0.3 for cement paste and between 0.1 and 0.3 for slag mortar which is in agreement with the results obtained by (Mohammad, Rahimi-Aghdam et al. 2018). As the duration of tests extends, the logarithmic evolution aligns closely with the experimental results, as observed in (Mallick, Anoop et al. 2019). Therefore, this study focuses on excluding the very early period, which may account for some of the disparities between the test results and the model predictions during this early age.

In Eq. 1, C [MPa] is a constant that depends on the concrete composition and $\tau$ [days or hours] is a parameter that depends on the age at loading $t_0$ [days or hours]. In case of incorporation of mineral additions, an additional term is needed to consider the influence of the mineral additions (Delsaute and Staquet 2020).

As, in Eq. 1, basic creep is described by a stress-linear rheological model consisting of one single dashpot, no creep recovery can be predicted. The authors' choice is to consider the easiest possible model that cor-

responds to the behaviour of the material under loading and that can be easily implemented in calculation codes. For stress histories involving partial or full unloading, a more advanced model is required. This model must be able to separate reversible and irreversible creep to correctly consider the phenomenon of recovery. In addition, if the stress level varies, the model must also be adapted to consider the consolidation stage reached during the previous loading which can affect the behaviour of concrete (Sellier, Multon et al. 2016).

In the first part of this paper, the results of a novel creep campaign that was conducted on four different concretes with a moderate loading time (in the range of 5 to 10 days) are presented and modelled using the logarithmic function (Eq. 1). The accuracy of the function is then analysed for previously published creep tests with shorter loading times. In the second part of the paper, rheological modelling, which is frequently used because it is straightforward to implement in FE models, is compared to the experimental results to evaluate their robustness. Indeed, rheological models are very useful tools that allow to fit the results of experimental creep tests (Bažant and Prasannan 1989), (De Schutter 1999), (Briffaut, Benboudjema et al. 2012). These models could be embedded in finite element modelling where, at each time step, the differential equation of the model is solved without storing all the history of the deformations at each Gauss point, see for example (Torrenti, Nedjar et al. 2023).

## 2. Experimental basic creep at early age

The constitutive relations at early age that are used to consider the principal ways in which temperature affects the kinetics of reactions are usually based on changes in the degree of hydration of the cementitious materials. Consequently, only creep tests where the degree of hydration ($\xi$) or the degree of heat development ($DoHd$) (De Schutter and Taerwe 1996) is known are considered in the present study. The degree of hydration corresponds to the fraction of the cement that has reacted, while the $DoHd$ corresponds to the ratio between the heat release at time t, $Q(t)$, that results from cement hydration and the maximum heat release from cement hydration $Q_{max}$ for a given water-to-cement ratio as indicated in Eq. 2. Both parameters can be linked if the heat release at complete hydration $Q_{tot}$ is known as shown in Eq. 2.

$$DoHd(t) = \frac{Q(t)}{Q_{max}} = \xi(t) \cdot \frac{Q_{tot}}{Q_{max}} \tag{2}$$

Furthermore, this study exclusively focuses on compressive creep tests. Numerous investigations have highlighted that creep behavior differs between compression and tension (Rossi, Charron et al. 2014). Specifi-

cally, it has been observed that creep is generally more pronounced in compression during the early age, while the reverse is true for later loading ages (Benboudjema, Briffaut et al. 2012). Rossi et al (Rossi, Charron et al. 2014) attribute these differences to two mechanisms: (1) the coupling between microcracking induced by specimen loading and additional water transfer, leading to additional self-drying shrinkage, and (2) the self-healing process also induced by microcracking. Those mechanisms result in additional shrinkage which will increase compressive creep strain and reduces tensile creep strain. While there are studies considering the aging of tensile creep function, knowledge in this area, especially at early ages, is scarce. Additionally, these studies lack information on the degree of hydration at the time of loading and during setting, to the best of the authors' knowledge.

Moreover, only linear creep is considered. The possibility of coupling with damage (Bazant 1995), (Cervera, Oliver et al. 1999), (Mazzotti and Savoia 2003), (Benboudjema, Meftah et al. 2005), (Rossi, Tailhan et al. 2012), (Saliba, Loukili et al. 2012) that could also exist at early age (Briffaut, Benboudjema et al. 2011), (Switek-Rey, Denarié et al. 2016), (Han, Xie et al. 2017), (Torrenti 2018) is not considered here, meaning that only linear creep tests have been selected. After a brief presentation of these tests, the results are compared to a prediction using Eq. 1. Table 1 presents all the concrete mixes that are tested with some properties.

Table 1 - Mixture proportions (kg/m³) and properties of the tested concretes

| | Bourchy | | | | Delsaute | | Briffaut |
|---|---|---|---|---|---|---|---|
| | R1 | G27 | C3 | G7 | Vercors | OC | |
| Cement type | CEM I | CEM II/A-LL | CEM I | CEM II/A-LL | CEM I | CEM I 52.5 N | CEM II/A-LL |
| Cement quantity (kg/m$^3$) | 410.0 | 316.8 | 360.0 | 90.0 | 320.0 | 340 | 350 |
| SCM type | - | SF | - | BFS | - | - | |
| SCM quantity (kg/m$^3$) | - | 43,2 | - | 270.0 | - | - | |
| Sand (kg/m$^3$) | 863.8 | 866.7 | 865.4 | 859.1 | 830 | 739 | 772 |
| Gravel (kg/m$^3$) | 958.7 | 1,059.4 | 1,057.7 | 1,050.0 | 995 | 1072 | 1100 |
| Plasticizer (kg/m$^3$) | - | 3.60 | 2.16 | 1.86 | 2.4 | - | 1,225 |
| Water (kg/m$^3$) | 188.6 | 150.3 | 160.2 | 160.4 | 170.9 | 184 | 201 |
| E at 28 days (GPa) | 39.0 | 44.0 | 41.8 | 41.6 | 35 | 40 | 33 |
| $f_c$ at 28 days (MPa) | 44.1 | 76.8 | 55.4 | 42.4 | 41 | 40 | 38 |
| Semi-adiabatic temperature rise (°C) | 35.8 | 18.9 | 18.7 | 7.7 | - | - | - |
| $\xi$ at setting (/) | 0.129 | 0.034 | 0.021 | 0.026 | 0.061 | 0.046 | 0.115 |

### 2.1. *Bourchy's tests (Bourchy 2018)*

During her PhD, Bourchy conducted a comprehensive examination of the early-age behavior of various concrete formulations (Bourchy 2018). This paper focuses on four distinct concrete mix designs, which are detailed in Table 1, denoted as concretes R1, G27, C3, and G7. These selections were made deliberately due to their diverse compositions and properties. R1 represents a conventional concrete previously used in Martin's study on Delayed Ettringite Formation (DEF) and composed of CEM I cement (Martin 2010). Notably, this formulation was designed to possess a high heat of hydration. The composition C3 also uses CEM I cement and it differs from the R1 formulation by exhibiting a lower heat of hydration. Both G27 and G7 compositions use the same CEM I cement as C3 but incorporate additional cementitious materials into their composition. Specifically, G27 incorporates a blended cement (consisting of 20% limestone) and maintains a silica fume-to-cement ratio of 12%. In contrast, G7 is produced using CEM I cement but incorporates a substantial 60% blast furnace slag content within the binder. These diverse concrete formulations were chosen to explore a wide spectrum of early-age behaviors, enabling a comprehensive analysis of their properties and performance in various conditions.

To evaluate these concrete formulations, the tests were performed in two steps. First, the evolution of the Young's modulus is measured since setting using a specially designed device named BTJASPE. A cylindrical specimen with a diameter of 100 mm and a height of 200 mm was manufactured. The device safeguards the concrete samples from desiccation by employing a protective mould since casting till the end of the test (Boulay, Staquet et al. 2013). A thermal regulation is incorporated in the mould and is set at 20 °C. Displacements were measured by using 3 LVDT sensors. The tests were carried out in a climate-controlled room at a temperature of 20 °C. Repeated loadings were applied by the testing device, involving the imposition of a consistent displacement during each loading, followed by a full unloading. Secondly, this apparatus enables to conduct creep tests, exerting a sustained load equivalent to 20% of the compressive strength on each concrete, for a minimum of four days. This testing procedure has been initiated between 8 and 14 days after casting, as described by Delsaute et al. (Delsaute, Boulay et al. 2016). For the purposes of this study, only compressive creep results are presented. The autogenous strain has been monitored in parallel with the BTJADE device (Delsaute and Staquet 2017) to define the creep strain.

Figure 2 shows the comparison between the experimental results and Eq. 1 (Model). Good agreement was obtained for all the concretes. The fitted parameters of Eq. 1 are presented in Table 2. The degree of hydration was estimated using a semi-adiabatic test (Briffaut, Benboudjema et al. 2012) and a maturity evolution based on the Arrhenius law.

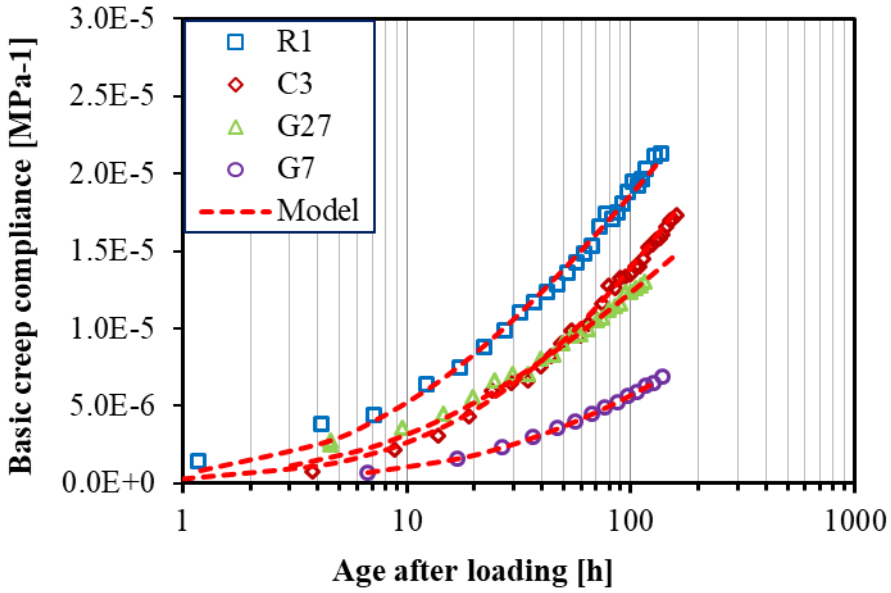


Figure 2 - Comparison between the Bourchy's experimental results and Eq. 1. The fitted parameters are set out in Table 2.

Table 2 - Parameters of Equation 1 for Bourchy's concretes

| R1 | | G27 | | C3 | | G7 | |
|---|---|---|---|---|---|---|---|
| $t_0$ (hours) = 312 | | $t_0$ (hours) = 194 | | $t_0$ (hours) = 252 | | $t_0$ (hours) = 343 | |
| $\xi(t_0) = 0.74$ | | $\xi(t_0) = 0.66$ | | $\xi(t_0) = 0.73$ | | $\xi(t_0) = 0.40$ | |
| C (GPa) | $\tau(t_0)$ (d) | C (GPa) | $\tau(t_0)$ (d) | C (GPa) | $\tau(t_0)$ (d) | C (GPa) | $\tau(t_0)$ (d) |
| 120 | 0.50 | 170 | 0.58 | 100 | 1.38 | 220 | 1.67 |

*2.2. Delsaute's tests: VeRCORs concrete (Delsaute, Torrenti et al. 2016)*

In the framework of nuclear safety and efforts to extend the service life of existing nuclear power plants in France, EDF (Electricité De France) has built a 1/3 scale experimental mock-up of a reactor containment building. The project is called VeRCORs and includes the study of the early age behaviour of cement-based materials (Charpin, Niepceron et al. 2021).

For the creep test, a cylindrical specimen with a diameter of 97 mm and a height of 350 mm was manufactured as well as a dummy specimen with the same dimensions for each test. After casting, all the specimens

were placed in a climate-controlled chamber at 20 °C and a relative humidity of 90%. The specimens were then demoulded, ground on both circular end faces and enclosed in two self-adhesive aluminium sheets to seal them. Compressive creep tests were performed on a frame designed at Université libre de Bruxelles (Delsaute, Boulay et al. 2016). A force cell was placed on the top of the sample. Displacements were measured with an extensometer consisting of two aluminium rings spaced 200 mm apart and three INVAR® rods onto which the three displacement sensors were fixed, 120° apart. The tests were carried out in a climate-controlled room at a temperature of 20 °C and relative humidity of 50%.

Compressive creep tests were carried out for different ages at loading: 19 h, 23 h, 43 h and 69 h. The load was kept constant for 17 days and the stress/strength ratio at the age at loading was 40%. For each age, tests were carried out on two specimens to ensure repeatability. The change in the specific creep is shown in Figure 3 for each age at loading and compared with a fitting of the parameters from Eq. 1 assuming that the parameter C is independent of the loading age. Table 3 gives the values of the fitted parameters. The parameters were fitted using a least square minimization of the difference between the experimental results. The degree of hydration was estimated by isothermal calorimetry at 20 °C. Figure 3 shows good agreement in the long term while, at very early age, a difference is apparent in the very short term.

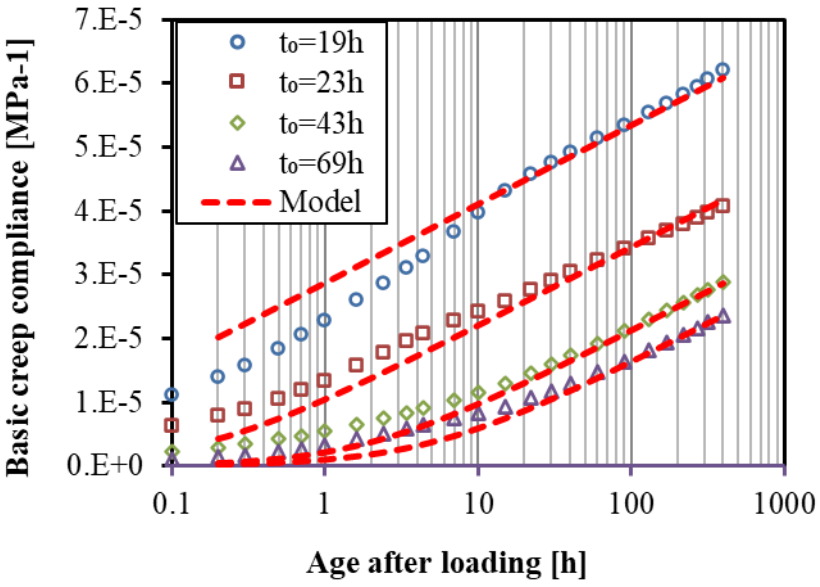


Figure 3 - Comparison between the Vercors's experimental results and Eq. 1. The fitted parameters are set out in Table 3

240 *2.3. Delsaute tests: ordinary concrete (Delsaute, Boulay et al. 2016)*

241 Delsaute, et al. also studied the basic creep at early age for an Ordinary Concrete (with a compressive
242 strength of 49 MPa at 28 days, as measured on a cube with 100 mm side). The same methodology that has
243 been presented in the previous section is used. Table 3 sets out the fitted creep parameters for this concrete
244 based on Eq. 1, and Figure 4 shows a comparison between the experimental results and modelling with this
245 equation. This shows good agreement, with a slight difference before 1 hour of loading.

246

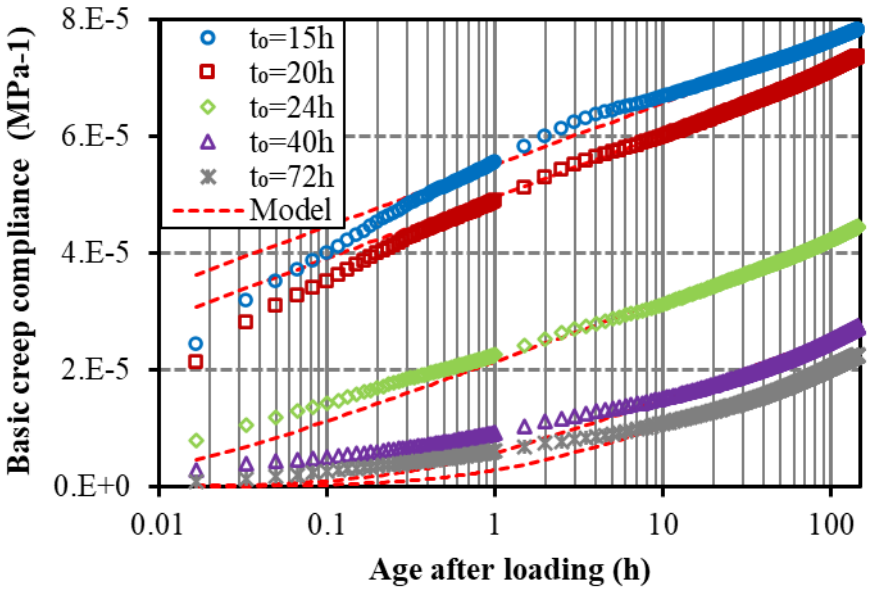


247

248 Figure 4 - Comparison between Delsaute's experimental results and Eq. 1. The fitted parameters are set out in
249 Table 3

250 *2.4. Briffaut's tests (Briffaut, Benboudjema et al. 2012)*

251 In the creep tests performed by Briffaut et al. (Briffaut, Benboudjema et al. 2012), the ages of loading
252 were between 24 h and 120 h. The loading level was less than 30% of the compressive strength at the age of
253 loading. The prismatic specimens measured 70x70x280 $mm^3$ and were placed in a temperature-controlled
254 room at 20 °C and protected from drying with a double-thickness self-adhesive aluminium sheath (a control
255 specimen was used to check that the sealing was sufficient for the duration of the tests) and loaded with a hy-
256 draulic loading frame. The strain measurements were performed on four generating lines to eliminate any
257 bending effects due to a slight possible decentering of the loading. Each measuring channel consisted of two 6
258 mm steel marbles spaced 200 mm apart. The strain was calculated by measuring the relative displacement of
259 the two marbles (performed with an LVDT). For each loading age, at least three specimens were tested. The

details of the experiments and the mix design of the concrete are presented in *(Briffaut, Benboudjema et al. 2012)* and in Table 1. The compressive strength at 28 days is 38 MPa. The degree of hydration was measured by semi-adiabatic tests and confirmed by measurement of the loss of ignition at 550°C (Briffaut, Benboudjema et al. 2012). Table 3 presents the fitted creep parameters for Eq. 1, and Figure 5 shows a comparison between the experimental results and modelling. This shows good agreement between both except during the first hours after loading.

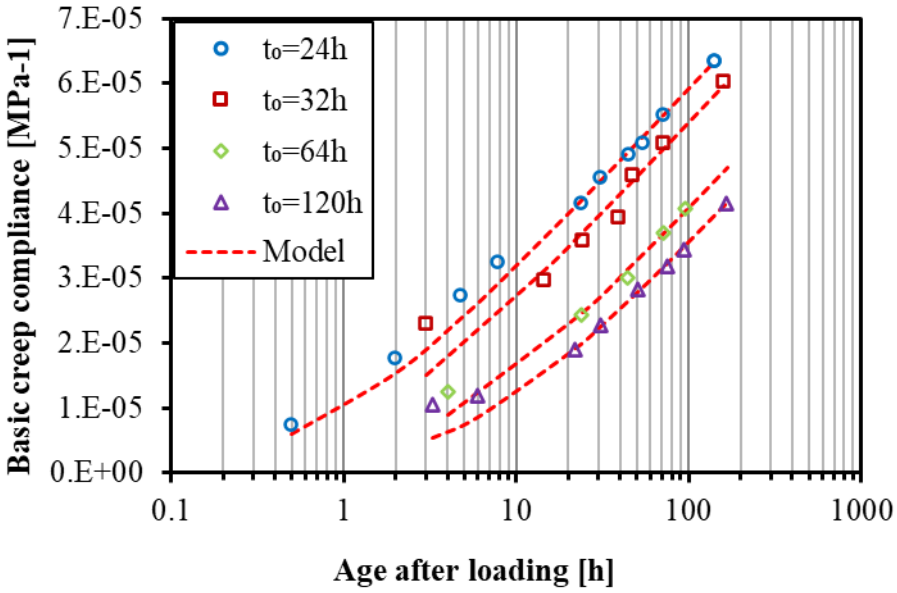


Figure 5 – Comparison between Briffaut's experimental results and Eq. 1. The fitted parameters are set out in Table 3

### *2.5. Conclusion*

The experimental results from the early age creep tests performed by several authors with different experimental devices and concrete mix designs show that early age creep follows a logarithmic course except, in some cases, at very early age during the first few hours after loading. This type of behaviour should therefore be used to model concrete at early age. Table 3 below summarises all the results obtained for the Vercors, OC and Briffaut compositions. The C parameter values vary significantly between the different compositions. According to the Model Code 2010, the value of C is linked to the compressive strength at 28 days. However, here, no correlation has been observed between C, $f_c$ or even E. In the next section, the practical implementation of this modelling is discussed.

Table 3 - Fitted parameters of Equation 1 for the Vercors, OC and Briffaut concretes

| Vercors concrete | |
|---|---|
| C (GPa) | 197 |

| $t_0$ (hours) | 19 | 23 | 43 | 69 |
|---|---|---|---|---|
| $\tau(t_0)$ (days) | 9.23E-5 | 5.04E-3 | 5.69E-2 | 1.55E-1 |
| $\xi(t_0)$ | 0.24 | 0.32 | 0.48 | 0.56 |
| OC | | | | |
| C (GPa) | 218 | | | |
| $t_0$ (hours) | 15 | 20 | 24 | 40 | 72 |
| $\tau(t_0)$ (days) | 2.49E-07 | 8.20E-07 | 3.90E-04 | 1.62E-02 | 4.76E-02 |
| $\xi(t_0)$ | 0.23 | 0.30 | 0.33 | 0.39 | 0.46 |
| Briffaut's concrete | | | | |
| C (GPa) | 93 | | | |
| $t_0$ (hours) | 24 | 32 | 64 | 120 |
| $\tau(t_0)$ (days) | 1.82E-02 | 3.02E-02 | 1.01E-01 | 1.58E-01 |
| $\xi(t_0)$ | 0.45 | 0.53 | 0.64 | 0.72 |

## 3. Modelling

Eq. 1 could of course be used in the framework of a finite element code with the assumption of the superposition principle. Nevertheless, dealing with such an equation and the superposition principle requires the entire stress history to be stored, for example at each Gauss point, leading to very long computation times (Hermerschmidt and Budelmann 2015). This explains why rheological models like a series of Kelvin-Voigt elements are very often used to predict creep in concrete (Bažant and Prasannan 1989), (Hauggaard, Damkilde et al. 1999).

Here, based on the microprestress theory (Bazant, Hauggaard et al. 1997), it was proposed to use a unique dashpot instead of a series of Kelvin-Voigt elements. If the viscosity $\eta$ of this dashpot changes linearly with time (Eq. 3), the integration of the strain $\varepsilon$ in a dashpot corresponds to Eq. 4:

$$\eta = C \cdot (t + \tau - t_0) \tag{3}$$

with C and $\tau$ are the parameters characterising the evolution of the viscosity.

$$\sigma = \eta \cdot \dot{\varepsilon} = C \cdot (t + \tau - t_0) \cdot \dot{\varepsilon} \Rightarrow d\varepsilon = \frac{\sigma \cdot dt}{C \cdot (\tau + t - t_0)} \Rightarrow \varepsilon = \frac{\sigma}{C} \cdot \ln\left(1 + \frac{t - t_0}{\tau}\right) \tag{4}$$

where $\sigma$ is the applied stress. The parameters C and $\tau$ of the dashpot can be fitted to the experimental results (as it was done in the first part of this paper, because Eqs. 1 and 4 are similar). To determine C, it is possible to perform a creep test on a hardened concrete. Micro-indentation can also be used to estimate this parameter (Vandamme and Ulm 2013), (Frech-Baronet, Sorelli et al. 2020). $\tau$ could also be estimated by creep tests.

Finally, it is also possible to evaluate this parameter by using the equation proposed by the fib model code MC2010 (Torrenti, Nedjar et al. 2023), for example, which has the form:

$$\tau(t_0) = \frac{1}{\left(0.035 + {}^{30}/_{t_0}\right)^2} \quad (5)$$

Where $t_0$ is expressed in days and varies depending on the type of cement, Figure 6 reveals that the equation fails to provide an accurate estimation of this parameter for all tested concretes during the early age. The parameter τ is consistently underestimated, except for the very early age. For comparison, results from previous studies by De Schutter (De Schutter 1999) and Gutsch (Gutsch 2000) have been included. It is generally observed that the evolution of τ does not adhere to a single trend when considering results based on the loading age during the very early age. However, at later ages, the development of τ remains relatively stable across different concrete compositions.

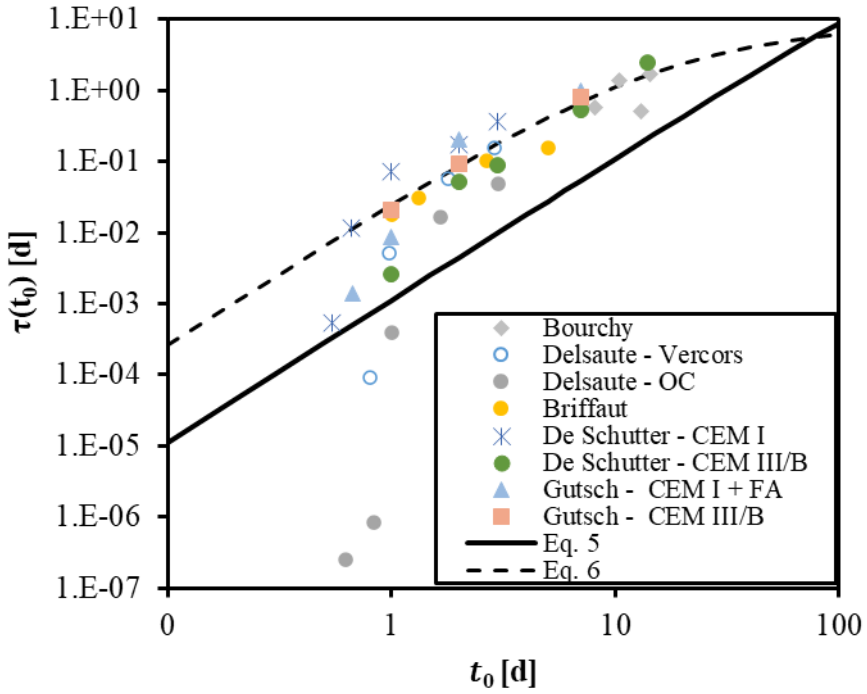


Figure 6 – $\tau(t_0)$ against $t_0$, including a comparative analysis with Equation 5 and Equation 6

Given the observations made from Figure 6 and aiming to enhance the prediction of τ, a new expression for $\tau$ in terms of loading age is proposed in Equation 6.

$$\tau(t_0) = \frac{0.052}{\left(0.078 + {}^{1.39}/_{t_0}\right)^2} \quad (6)$$

Where $t_0$ is expressed in days. Equation 6 is compared to experimental results and Equation 5 in Figure 6. As anticipated, Equation 6 demonstrates an improved overall alignment with loading ages across ages at loading higher than 1 day. However, it is noteworthy that Equation 5 more accurately replicates τ values at a very early age. To quantitatively assess the performance of Equations 5 and 6, errors derived from both equations are calculated and presented in Table 4 for the compositions outlined in sections 2.2 to 2.4. The error is computed based on the sum of the squares of the differences obtained. Illustratively, the outcomes of Equations 5 and 6 are depicted in Figure 7. It becomes evident that neither of the two equations can predict basic creep at both very early and older ages.

Table 4 – Performance evaluation of Equations 5 to 7: error analysis

| | **Error** | | | |
|---|---|---|---|---|
| | Eq. 5 | Eq. 6 | Eq. 7 / Case A | Eq. 7 / Case B |
| OC | 1.61E-07 | 1.65E-06 | 9.40E-08 | 1.05E-07 |
| Vercors | 1.39E-08 | 1.33E-08 | 7.53E-10 | 1.45E-09 |
| Briffaut | 2.42E-09 | 8.51E-10 | 1.58E-10 | 1.68E-10 |

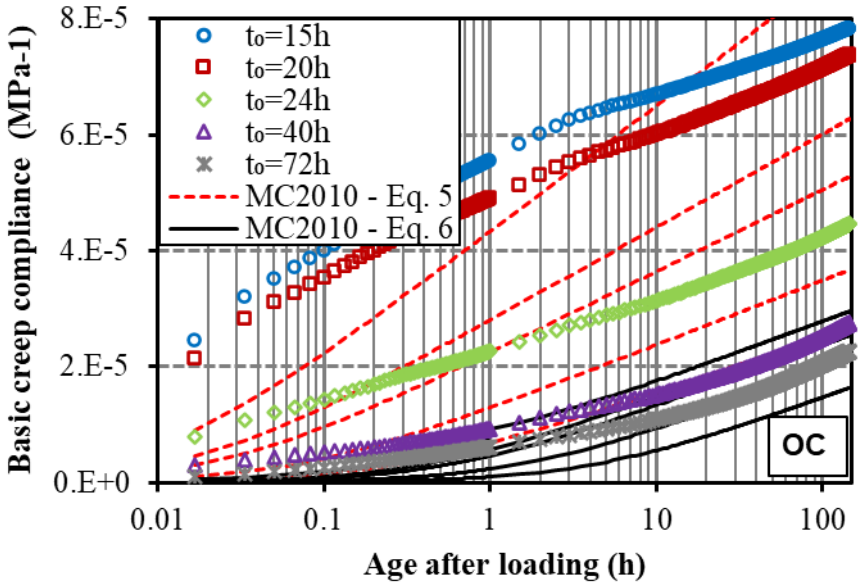

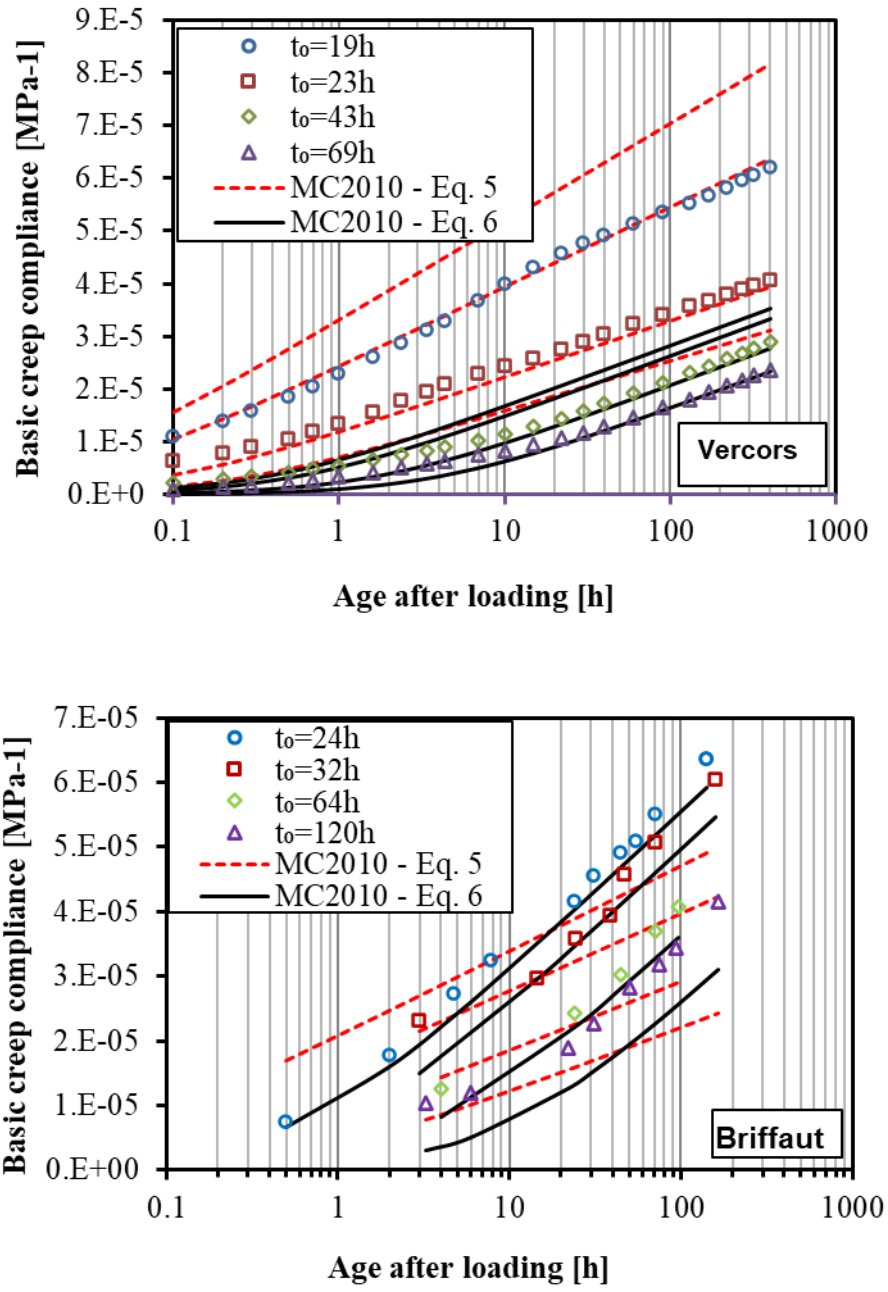


Figure 7 – Performance evaluation of Equation 5 to 6 on the OC (a), Vercors (b) and Briffaut's (c) concrete compositions.

318 As indicated in section 2, the maturity of cement-based materials can also be expressed by means of the
319 degree of hydration. Figure 8 shows how the parameter τ varies according to the degree of hydration.

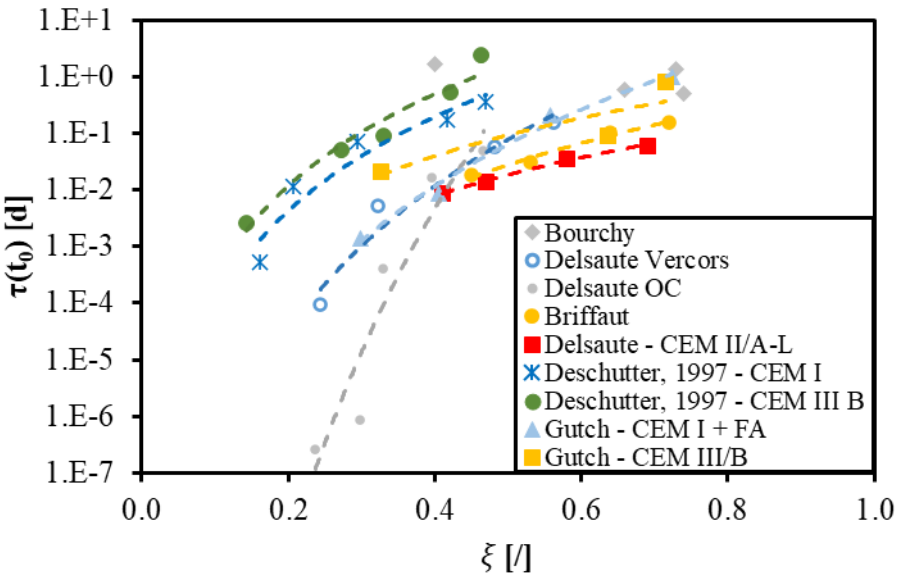


Figure 8 - $\tau(t_0)$ against $\xi$. Dashed lines delineate the power trend line.

It is apparent that the relationship between both parameters differ for different concretes. It can be mainly observed that:

- A shift is observed in the development of $\tau$ between the different compositions.
- The relationship between $\tau$ and $\xi$ follows a power trend.

One notable distinction among various shifts in $\tau$ concerning the degree of hydration lies in the initiation point of the curve, exhibiting considerable variability across compositions. This divergence is attributed to the fact that, for certain compositions, the material undergoes setting at a significantly lower degree of hydration compared to others. This underscores the importance of accounting for the degree of hydration at the time of setting $\xi_0$ when modelling $\tau$. Figure 9 presents the results for $\tau$ as a function of $\xi - \xi_0$, revealing a dispersion of outcomes, particularly during the very early age when the degree of hydration is low. No discernible trend is observed between the nature (e.g., type of cement, water-cement ratio, etc.) or performance characteristics (e.g., compressive strength) of the compositions and the relationship between $\tau$ and $\xi - \xi_0$. This fact is discussed at the end of the section.

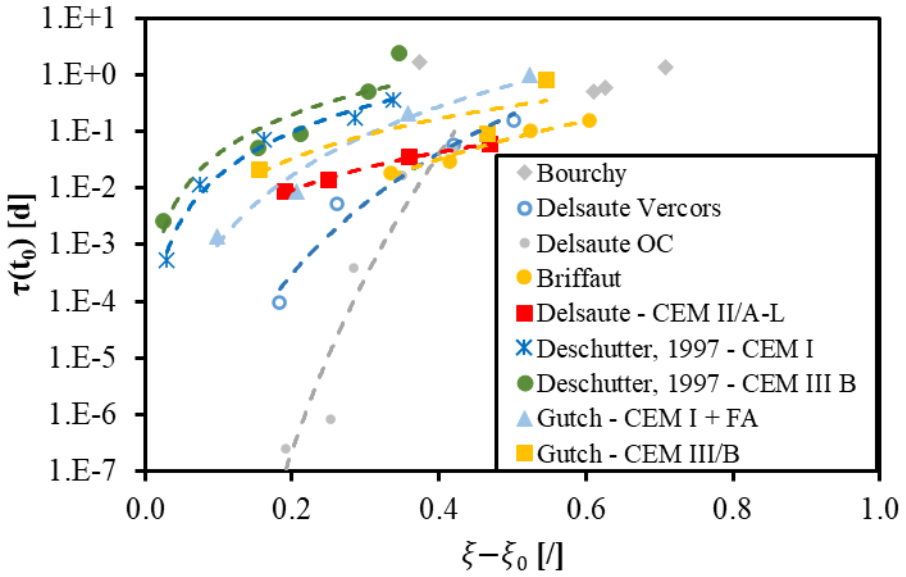


Figure 9 - Plot of $\tau(t_0)$ against $\xi$- $\xi_0$. The dashed lines delineate the power trend line.

The τ values at the time of setting exhibit notable variations among different compositions when attempting to extrapolate the obtained results. However, the τ value at the time of loading is directly linked to concrete viscosity through the parameter C (see Eq. 3). Although the viscosity of concrete at the time of setting is unknown, it is considerably lower than the measured values in the studied concretes. Given the substantial fluctuations in τ at the time of setting, it becomes evident that, during and shortly after setting, the τ value is prone to significant underestimation or overestimation, depending on the situation. This can lead to a pronounced over- or under-estimation of the creep phenomenon in the initial hours post-setting. To address this, the model should incorporate a minimum value for τ at the time of setting. For fresh concrete, the plastic viscosity can vary between 20 and 800 Pa.s (Chidiac and Mahmoodzadeh 2009). By comparison, water has a viscosity of 0.002 Pa.s. Assuming a τ value of 2.49E-7 day and a C value of 218 GPa, the resulting viscosity at the time of loading is estimated to be 4.69E9 Pa.s. This value surpasses the viscosity of fresh concrete by more than 1E6 times. Conversely, in the opposite scenario, considering a plastic viscosity of 1000 Pa.s and the same C value, the resulting τ is estimated to be 5.31E-14 day. This value could be considered as a lower bound of τ. However, for a more accurate estimation of τ at the setting time, additional data is needed. One method to estimate this value involves using oscillatory shear during the fresh stage until setting (Banfill 1991). Consequently, it is reasonable to assume that this lower threshold value will have minimal impact on the subsequent development of τ. It is crucial to note that this study focuses on the material's behaviour from the time of setting, and

thus, the data from this study cannot be applied before the material has set. Considering these observations, a new relationship between τ and the degree of hydration is proposed in Equation 7:

$$\tau = \tau_0 + a \cdot (\xi - \xi_0)^b \text{ for } \xi > \xi_0 \quad (7)$$

Where $\tau_0$ corresponds to the value of $\tau$ at final setting time and is expressed in day, $a$ and $b$ are dimensionless material parameters and are presented in Table 5. In this case, for an accurate evaluation of early age creep, at least two creep tests for two different $\xi_0$ are needed.

Table 5 – Fitted parameters and resulting $R^2$ from Eq. 7

| | | | Case A: all data | | | Case B: data from 2 tests | | |
|---|---|---|---|---|---|---|---|---|
| | $\xi_0$ | C [MPa] | a | b | $R^2$ | a | b | $R^2$ |
| Deschutter, 1997 - CEM I | 0.132 | 159498 | 5.98 | 2.56 | 0.96 | 6.65 | 2.68 | 0.97 |
| Deschutter, 1997 - CEM III/B | 0.118 | 118861 | 7.65 | 2.27 | 0.74 | 38.42 | 2.60 | 0.77 |
| Delsaute, 2017 - OC - CEM I | 0.046 | 217846 | 338688.20 | 17.41 | 0.91 | 28826.24 | 15.41 | 0.92 |
| Delsaute, 2016 - Vercors - CEM I | 0.061 | 196000 | 27.00 | 7.08 | 0.99 | 24.67 | 7.36 | 0.99 |
| Delsaute, 2019 - CEM II/A-L | 0.220 | 180000 | 0.33 | 2.22 | 1.00 | 0.31 | 2.16 | 1.00 |
| Briffaut, 2010 - CEM II/A-LL | 0.115 | 93190 | 1.09 | 3.84 | 0.99 | 0.99 | 3.65 | 0.99 |
| Gutsch, 2000 - CEM I + FA | 0.200 | 104970 | 10.92 | 4.03 | 1.00 | 12.64 | 3.92 | 1.00 |
| Gutsch, 2000 - CEM III/B | 0.170 | 88131 | 1.43 | 2.34 | 0.64 | 4.77 | 2.93 | 0.69 |

Equation 7 is compared to experimental results in Figure 10. For every age at loading, a good agreement is obtained between the experimental results and Equation 7. To quantitatively assess the performance of Equations 7, the error is calculated, as for Equation 5 and 6 previously, and is presented in Table 4. It appears that the error is strongly reduced by using Equation 7 and data from Table 5 (case A). While this model effectively captures the aging of the creep function, noticeable variations in the coefficients $a$ and $b$ are observed across different compositions. The parameter $a$ ranges between 1.09 and 338688, while the parameter $b$ varies between 2.22 and 17.41. Despite the inherent differences in compositions due to binder nature and admixture presence, the expectation was for these variations to be smaller. Notably, the OC composition stands out from the rest. Excluding this data, the parameter $a$ varies between 1.09 and 27.00, and the parameter $b$ varies between 2.22 and 7.08, indicating significantly narrower ranges.

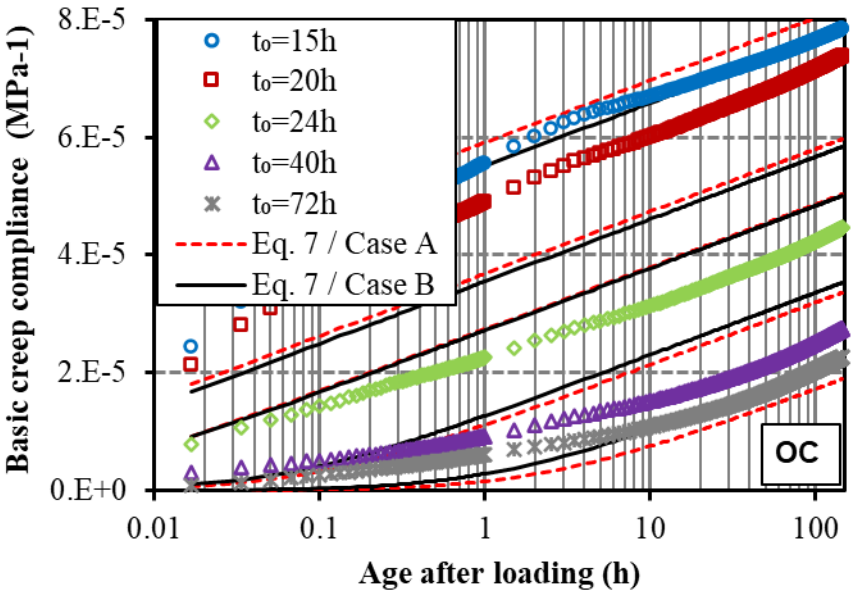
8.E-5
6.E-5
4.E-5
2.E-5
0.E+0
Basic creep compliance (MPa-1)
to=15h
to=20h
to=24h
to=40h
to=72h
Eq. 7 / Case A
Eq. 7 / Case B
OC
0.01
0.1
1
10
100
Age after loading (h)

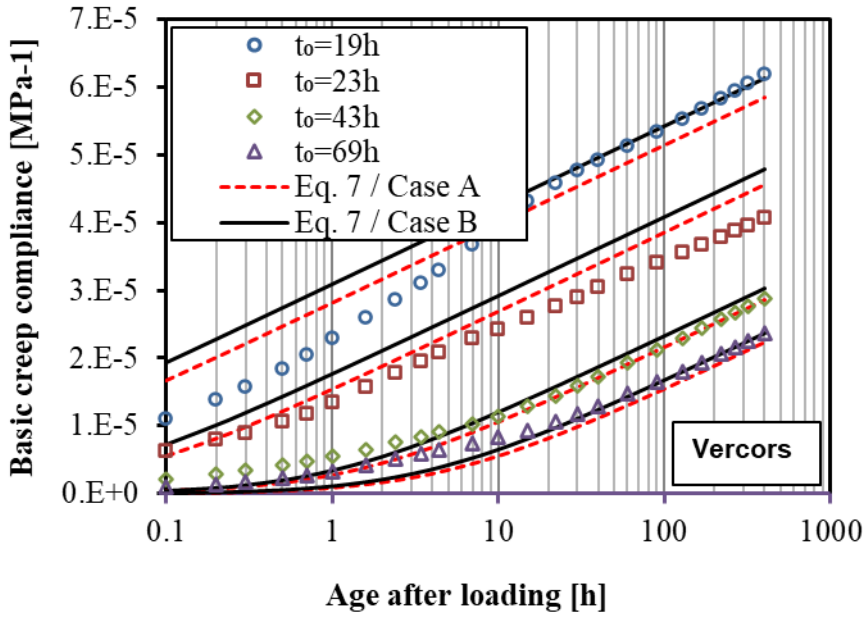
7.E-5
6.E-5
5.E-5
4.E-5
3.E-5
2.E-5
1.E-5
0.E+0
Basic creep compliance [MPa-1]
to=19h
to=23h
to=43h
to=69h
Eq. 7 / Case A
Eq. 7 / Case B
Vercors
0.1
1
10
100
1000
Age after loading [h]

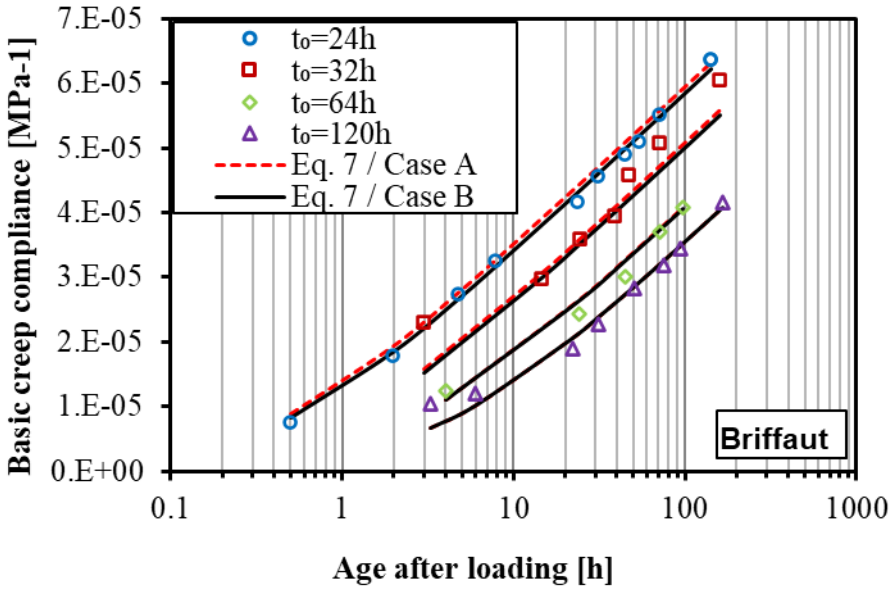


Figure 10 – Performance evaluation of Equation 7 on the OC (a), Vercors (b) and Briffaut's (c) concrete compositions for cases A and B.

These substantial variations can be attributed to the inclusion of data from multiple laboratories at different times, employing diverse technologies and test protocols. Moreover, significant disparities arise in determining fundamental parameters such as the degree of hydration (measured by isothermal calorimetry, semi-adiabatic calorimetry, or adiabatic calorimetry) and the final setting time (determined through ultrasonic measurement or based on a mechanical percolation threshold linked to compressive or tensile strength or modulus of elasticity). The devices and the geometry of the samples used in those studies are also different. The impacts of these differences are challenging to quantify, underscoring the need to establish consistent protocols across laboratories for characterizing and modelling the aging of the creep function.

This also highlights the challenges posed by existing databases, including those proposed by Bazant's team (Mija H. Hubler and Zdenek), as previously indicated by (Rasoolinejad, Rahimi-Aghdam et al. 2018). While it may be impractical to establish a universal relationship between the degree of hydration and the parameter $\tau$, which represents the aging factor of the creep function, this work demonstrates that these two parameters are connected by a power law. Hence, it appears that such a simple law can be characterized with just 2 short-duration tests (< 1 month) conducted at sufficiently spaced degrees of hydration. To directly validate this assertion, parameters $a$ and $b$ in Equation 7 are computed using the $\tau$ data acquired for the first and last loading ages across different datasets. The corresponding results are presented in Table 5 (case B). Notably, it is ob-

served that the values for coefficients $a$ and $b$ closely align with those obtained from the comprehensive data-set (case A). This close agreement is further illustrated in Figure 10, demonstrating a high degree of concordance. Furthermore, through the assessment of the calculated error, it appears that the error increases by 21.3% when relying on 2 tests instead of 4 to 5 tests for determining the aging of $\tau$ as a function of the $\xi - \xi_0$.

Finally, it was observed that the proposed model is unable to accurately fit the initial hours of loading and tends to underestimate the creep function. This discrepancy is particularly noticeable when loading is conducted at a very early age. It appears that during the initial 3 hours of loading, the creep function follows a power law with the exponent $n$ varying between 0.15 and 0.60. An average value of 0.33 is determined. Figure 11 illustrates all the obtained results. For a more precise modelling of creep behaviour from loading, this observed power-law behavior could be considered, as proposed in more complex models that account for multiple creep components (see, for example, (Delsaute, Torrenti et al. 2017)).

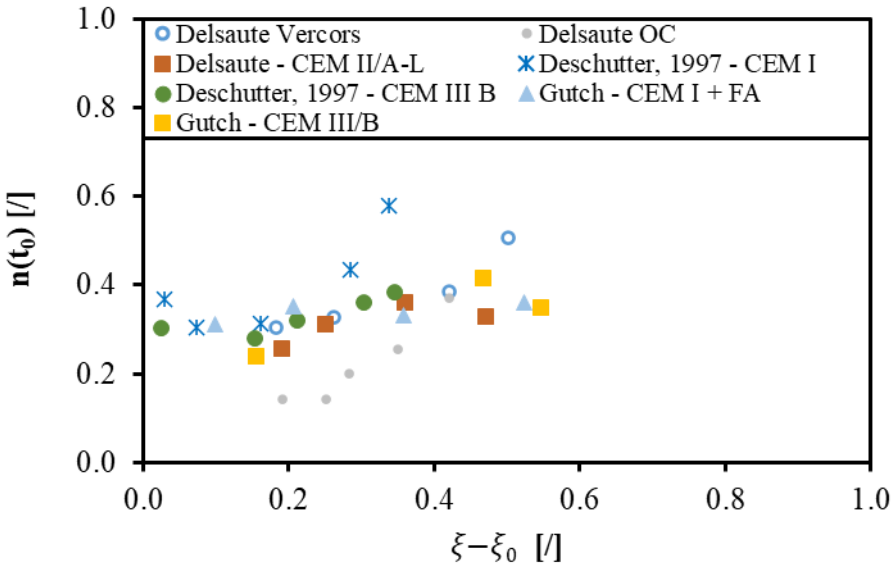


Figure 11 –Power law exponent n($t_0$) against $\xi$- $\xi_0$

## 4. Conclusions

This study analyses the basic creep of various concrete mixes for several ages at loading, especially at very early age ($t_0$ < 24h) and early age ($t_0$ < 28 days). It is shown that:

- A logarithmic expression that contains two parameters that describe the material (C and $\tau$) can accurately model basic creep from very early age except for the first hours of loading. Parameter C relates to the amplitude of creep and depends solely on the composition of the concrete. The other parameter τ relates to the kinetics of creep and depends on the age of the material at loading and the nature of the concrete mixture.
- The logarithmic expression corresponds to a rheological model consisting of a single dashpot for which viscosity changes linearly with time. This model has the advantage that it removes the need to store the entire stress history to compute the stress generated by the restraint of free deformation which greatly reduces computation time.
- The material ageing parameter τ varies according to a power law when plotted according to the degree of hydration. This relationship depends on the composition. At least two compressive creep tests performed at two different degrees of hydration are needed to calibrate the material parameters and consider the effect of ageing on basic creep compliance.
- Furthermore, the introduction of a new relationship (Equation 7) between creep and degree of hydration represents a significant advancement in modelling accuracy. This relationship, which reduces error and aligns more closely with experimental results, underscores the importance of accounting for the degree of hydration at the age of loading and the time at setting. The proposal of material parameters (a and b) within Equation 7, while showing substantial variation across different compositions, emphasizes the challenges posed by diverse testing methodologies and the need for standardized protocols in concrete testing and modelling.
- The initial development of the basic creep compliance (< 3 hours of loading) follows a power trend with an average exponent of 0.33.

This study deals only with basic compressive creep for moderate levels of stress and for a curing temperature of 20 °C. Further studies are needed to assess cracking risks at early age, for example by investigating basic tensile creep and the influence of the curing temperature, stress level, drying and creep recovery.

## References


Atrushi, D. S. (2003). Tensile and compressive creep of early age concrete: Testing and modelling Thesis, PhD Thesis, Norwegian University of Sciences and Technology.

Azenha, M., F. Kanavaris, D. Schlicke, A. Jędrzejewska, F. Benboudjema, T. Honorio, V. Šmilauer, C. Serra, J. Forth, K. Riding, B. Khadka, C. Sousa, M. Briffaut, L. Lacarrière, E. Koenders, T. Kanstad, A. Klausen, J.-M. Torrenti and E. M. R. Fairbairn (2021). "Recommendations of RILEM TC 287-CCS: thermo-chemo-mechanical modelling of massive concrete structures towards cracking risk assessment." Materials and Structures **54**(4): 135.

Banfill, P. F. G. (1991). Rheology of fresh cement and concrete.

Bazant, Z. P. (1995). "Creep and shrinkage prediction model for analysis and design of concrete structures - Model B-3." Materials & Structures **28**: 357-365.

Bazant, Z. P., A. Hauggaard, S. Baweja and F.-J. Ulm (1997). "Microprestress-solidification theory for concrete creep. I. Aging and drying effects." J. Eng. Mech. **123**: 1188-1194.

Bažant, Z. P. and S. Prasannan (1989). "Solidification theory for concrete creep. II: Verification and application." Journal of Engineering mechanics **115**(8): 1704-1725.

Benboudjema, F., M. Briffaut, A. Hilaire, J. M. Torrenti and G. Nahas (2012). Early Age Behavior of Massive Concrete Structures: From Experiments To Numerical Simulations. CONCRACK 3-RILEM-JCI International Workshop on Crack Control Mass Concrete and Related Issues Concerning Early-Age of Concrete Structures. Paris, France**:** 1-12.

Benboudjema, F., J. Carette, B. Delsaute, T. Honorio de Faria, A. Knoppik, L. Lacarrière, A. Neiry de Mendonça Lopes, P. Rossi and S. Staquet (2019). Mechanical Properties. Thermal Cracking of Massive Concrete Structures: State of the Art Report of the RILEM Technical Committee 254-CMS. E. M. R. Fairbairn and M. Azenha. Cham, Springer International Publishing**:** 69-114.

Benboudjema, F., F. Meftah and J. M. Torrenti (2005). "Interaction between drying, shrinkage, creep and cracking phenomena in concrete." Engineering Structures **27**(2): 239-250.

Benboudjema, F. and J. M. Torrenti (2008). "Early age behaviour of concrete nuclear containments." Nuclear Engineering and Design **238**: 2495-2506.

Binder, E., M. Königsberger, R. Díaz Flores, H. A. Mang, C. Hellmich and B. L. A. Pichler (2023). "Thermally activated viscoelasticity of cement paste: Minute-long creep tests and micromechanical link to molecular properties." Cement and Concrete Research **163**: 107014.

Boulay, C., S. Staquet, B. Delsaute, J. Carette, M. Crespini, O. Yazoghli-Marzouk, E. Merliot and S. Ramanich (2013). "How to monitor the modulus of elasticity of concrete, automatically since the early age?" Materials and Structures.

Bourchy, A. (2018). Relation chaleur d'hydratation du ciment : montée en température et contraintes générées au jeune âge du béton, These de l'Universite Paris-Est.

Briffaut, M., F. Benboudjema, J.-M. Torrenti and G. Nahas (2012). "Concrete early age basic creep: Experiments and test of rheological modelling approaches." Construction and Building Materials **36**: 373-380.

Briffaut, M., F. Benboudjema, J. M. Torrenti and G. Nahas (2011). "Numerical analysis of the thermal active restrained shrinkage ring test to study the early age behavior of massive concrete structures." Engineering Structures **33**(4): 1390-1401.

Briffaut, M., F. Benboudjema, J. M. Torrenti and G. Nahas (2012). "Analysis of semi-adiabiatic tests for the prediction of early-age behavior of massive concrete structures." Cement and Concrete Composites **34**(5): 634-641.

CEN (2023). prEN 1992-1-1:2023, Eurocode 2: Design of concrete structures — Part 1-1: General rules — Rules for buildings, bridges and civil engineering structures.

Cervera, M., J. Oliver and T. Prato (1999). "Thermo-chemo-mechanical model for concrete. II: Damage and creep." Journal of engineering mechanics **125**(9): 1028-1039.

Charpin, L., J. Niepceron, M. Corbin, B. Masson, J.-P. Mathieu, J. Haelewyn, F. Hamon, M. Åhs, S. Aparicio, M. Asali, B. Capra, M. Azenha, D. E. M. Bouhjiti, K. Calonius, M. Chu, N. Herrman, X. Huang, S. Jiménez, J. Mazars, M. Mosayan, G. Nahas, J. Stepan, T. Thenint and J.-M. Torrenti (2021). "Ageing and air leakage assessment of a nuclear reactor containment mock-up: VERCORS 2nd benchmark." Nuclear Engineering and Design **377**: 111136.

Chidiac, S. E. and F. Mahmoodzadeh (2009). "Plastic viscosity of fresh concrete – A critical review of predictions methods." Cement and Concrete Composites **31**(8): 535-544.

Dabarera, A., L. Li and V. Dao (2021). "Experimental evaluation and modelling of early-age basic tensile creep in high-performance concrete." Materials and Structures **54**(3): 130.

De Schutter, G. (1999). "Degree of hydration based Kelvin model for the basic creep of early age concrete." Materials and Structures **32**: 260-265.
De Schutter, G. and L. Taerwe (1996). "Degree of hydration-based description of mechanical properties of early age concrete." Materials & Structures **29**(190): 335-344.
Delsaute, B., C. Boulay and S. Staquet (2016). "Creep testing of concrete since setting time by means of permanent and repeated minute-long loadings." Cement and Concrete Composites **73**: 75-88.
Delsaute, B. and S. Staquet (2017). "Decoupling Thermal and Autogenous Strain of Concretes with Different Water/Cement Ratios During the Hardening Process." Advances in Civil Engineering Materials **6**(2): 1-22.
Delsaute, B. and S. Staquet (2019). "Development of strain-induced stresses in early age concrete composed of recycled gravel or sand." J. Adv. Concr. Technol. **17**.
Delsaute, B. and S. Staquet (2020). Monitoring the Viscoelastic Behaviour of Cement Based Materials by Means of Repeated Minute-Scale-Duration Loadings. Advanced Techniques for Testing of Cement-Based Materials. M. Serdar, I. Gabrijel, D. Schlicke, S. Staquet and M. Azenha. Cham, Springer International Publishing**:** 99-134.
Delsaute, B. and S. Staquet (2020). Testing Concrete Since Setting Time Under Free and Restrained Conditions. Advanced Techniques for Testing of Cement-Based Materials. M. Serdar, I. Gabrijel, D. Schlicke, S. Staquet and M. Azenha. Cham, Springer International Publishing**:** 177-209.
Delsaute, B., J. M. Torrenti and S. Staquet (2016). Monitoring and modeling of the early age properties of the Vercors Concrete. TINCE 2016, Paris. Paris, France**:** 12.
Delsaute, B., J. M. Torrenti and S. Staquet (2017). "Modeling basic creep of concrete since setting time." Cement and Concrete Composites **83**(Supplement C): 239-250.
Fairbairn, E. M. R. and M. Azenha (2019). Thermal Cracking of Massive Concrete Structures, Springer International Publishing, Cham.
Frech-Baronet, J., L. Sorelli and J. P. Charron (2017). "New evidences on the effect of the internal relative humidity on the creep and relaxation behaviour of a cement paste by micro-indentation techniques." Cement and Concrete Research **91**: 39-51.
Frech-Baronet, J., L. Sorelli and Z. Chen (2020). "A closer look at the temperature effect on basic creep of cement pastes by microindentation." Construction and Building Materials **258**: 119455.
Gawin, D., F. Pesavento and B. A. Schrefler (2006). "Hygro- thermo- chemo- mechanical modelling of concrete at early ages and beyond. Part II: shrinkage and creep of concrete." International journal for numerical methods in engineering **67**(3): 332-363.
Ghasabeh, M. and S. Göktepe (2023). "Phase-field modeling of thermal cracking in hardening mass concrete." Engineering Fracture Mechanics **109398**.
Gutsch, A. W. (2000). Stoffeigenschaften jungen Betons – Versuche und Modelle.
Han, B., H.-B. Xie, L. Zhu and P. Jiang (2017). "Nonlinear model for early age creep of concrete under compression strains." Construction and Building Materials **147**: 203-211.
Hanson, J. A. (1953). A 10-year study of creep properties of concrete, Report SP-38. Design and Construction Division.
Hauggaard, A., L. Damkilde and P. F. Hansen (1999). "Transitional thermal creep of early age concrete." Journal of materials in civil engineering **125**: 458-465.
Hermerschmidt, W. and H. Budelmann (2015). Creep of Early Age Concrete under Variable Stress. CONCREEP 10, American Society of Civil Engineers, Reston, VA, USA.
Hilaire, A., F. Benboudjema, A. Darquennes, Y. Berthaud and G. Nahas (2014). "Modeling basic creep in concrete at early-age under compressive and tensile loading." Nuclear Engineering and Design **269**: 222-230.
Irfan-ul-Hassan, M., M. Königsberger, R. Reihsner, C. Hellmich and B. Pichler (2017). "How water-aggregate interactions affect concrete creep: Multiscale analysis." Journal of Nanomechanics and Micromechanics **7**(4): 04017019.
Irfan-ul-Hassan, M., B. Pichler, R. Reihsner and C. Hellmich (2016). "Elastic and creep properties of young cement paste, as determined from hourly repeated minute-long quasi-static tests." Cement and Concrete Research **82**: 36-49.
Jiang, C., Y. Yang, Y. Wang, Y. Zhou and C. Ma (2014). "Autogenous shrinkage of high performance concrete containing mineral admixtures under different curing temperatures." Construction and Building Materials **61**: 260-269.
Khan, I., A. Castel and R. I. Gilbert (2017). "Tensile creep and early-age concrete cracking due to restrained shrinkage." Construction and Building Materials **149**: 705-715.
Klausen, A. E., T. Kanstad, Ø. Bjøntegaard and E. Sellevold (2017). "Comparison of tensile and compressive creep of fly ash concretes in the hardening phase." Cement and Concrete Research **95**: 188-194.

Klemczak, B. and A. Knoppik-Wróbel (2015). "Reinforced concrete tank walls and bridge abutments: Early-age behaviour, analytic approaches and numerical models." Engineering Structures **84**: 233-251.
Lacarriere, L., A. Sellier, P. Souyris, B. Kolani and P. Chhun (2020). "Numerical prediction of cracking risk of reinforced concrete structures at early age." RILEM Technical Letters **5**(0): 41-55.
Lackner, R. and H. A. Mang (2004). "Chemoplastic material model for the simulation of early-age cracking: From the constitutive law to numerical analyses of massive concrete structures. ." Cement and Concrete Composites **26**(5): 551-562.
Larson, M. and J. E. Jonasson (2003). "Linear logarithmic model for concrete creep I. formulation and evaluation." Journal of Advanced Concrete Technology **1**(2): 172-187.
Leroy, R., F. Le Maou and J. M. Torrenti (2017). "Long term basic creep behavior of high performance concrete. Data and Modelling." Materials & Structures: 50-85.
Liu, Y., Y. Wei, L. Ma and L. Wang (2022). "Restrained shrinkage behavior of internally-cured UHPC using calcined bauxite aggregate in the ring test and UHPC-concrete composite slab." Cement and Concrete Composites **134**: 104805.
Mallick, S., M. B. Anoop and K. B. Rao (2019). "Early age creep of cement paste-Governing mechanisms and role of water-A microindentation study." Cement and Concrete Research **116**: 284-298.
Martin, R. P. (2010). Analyse sur structures modèles des effets mécaniques de la réaction sulfatique interne du béton Thesis, Thèse de l'Université de Paris-Est.
Mazzotti, C. and M. Savoia (2003). "Nonlinear creep damage model for concrete under uniaxial compression." Journal of engineering mechanics **129**(9): 1065-1075.
Mija H. Hubler, R. W. and P. B. Zdenek "Comprehensive Database for Concrete Creep and Shrinkage: Analysis and Recommendations for Testing and Recording." ACI Materials Journal **112**(4).
Mohammad, R., S. Rahimi-Aghdam and Z. P. Bažant (2018). "Statistical filtering of useful concrete creep data from imperfect laboratory tests." Materials and Structures **51**: 1-14.
Muller, H. S., I. Anders, R. Breiner and M. Vogel (2013). "Concrete: treatment of types and properties in fib Model Code 2010." Structural Concrete **14**: 320–334.
Naqi, A., B. Delsaute, M. Königsberger and S. Staquet (2023). "Monitoring early age elastic and viscoelastic properties of alkali-activated slag mortar by means of repeated minute-long loadings." Developments in the Built Environment **16**: 100275.
Østergaard, L., D. A. Lange, S. A. Altoubat and H. Stang (2001). "Tensile basic creep of early-age concrete under constant load." Cement and Concrete Research **31**(12): 1895-1899.
Ranaivomanana, N., S. Multon and A. Turatsinze (2013). "Basic creep of concrete under compression, tension and bending." Construction and Building Materials **38**(Supplement C): 173-180.
Rasoolinejad, M., S. Rahimi-Aghdam and Z. P. Bažant (2018). "Statistical filtering of useful concrete creep data from imperfect laboratory tests." Materials and Structures **51**(6): 153.
Rossi, P., J. P. Charron, M. Bastien-Masse, J.-L. Tailhan, F. Le Maou and S. Ramanich (2014). "Tensile basic creep versus compressive basic creep at early ages: comparison between normal strength concrete and a very high strength fibre reinforced concrete." Materials and Structures **47**(10): 1773-1785.
Rossi, P., J.-L. Tailhan and F. Le Maou (2013). "Comparison of concrete creep in tension and in compression: Influence of concrete age at loading and drying conditions." Cement and Concrete Research **51**(Supplement C): 78-84.
Rossi, P., J.-L. Tailhan, F. Le Maou, L. Gaillet and E. Martin (2012). "Basic creep behavior of concretes investigation of the physical mechanisms by using acoustic emission." Cement and Concrete Research **42**(1): 61-73.
Saliba, J., A. Loukili, F. Grondin and J. P. Regoin (2012). "Experimental study of creep-damage coupling in concrete by acoustic emission technique." Materials and Structures **45**(9): 1389-1401.
Sellier, A., S. Multon, L. Buffo-Lacarrière, T. Vidal, X. Bourbon and G. Camps (2016). "Concrete creep modelling for structural applications: non-linearity, multi-axiality, hydration, temperature and drying effects." Cement and Concrete Research **79**: 301-315.
Su, X., M. Jia, Y. Wu, L. Yao and W. Xu (2023). "A hierarchical creep model for cement paste: From decoding nano-microscopic CSH creep to considering microstructure evolution." Journal of Building Engineering: 107606.
Suwanmaneechot, P., A. Aili and I. Maruyama (2020). "Creep behavior of CSH under different drying relative humidities: Interpretation of microindentation tests and sorption measurements by multi-scale analysis." Cement and Concrete Research **132**: 106036.
Switek-Rey, A., E. Denarié and E. Brühwiler (2016). "Early age creep and relaxation of UHPFRC under low to high tensile stresses." Cement and Concrete Research **83**: 57-69.

Torrenti, J.-M., B. Nedjar and A. Aili (2023). Dependence of Basic Creep on the Relative Humidity. Building for the Future: Durable, Sustainable, Resilient, Cham, Springer Nature Switzerland.
Torrenti, J. M. (2018). "Basic creep of concrete-coupling between high stresses and elevated temperatures." European Journal of Environmental and Civil Engineering **22**(12): 1419-1428.
Ulm, F. J., F. Le Maou and C. Boulay (1999). "Creep and shrinkage coupling: new review of some evidence." Revue française de génie civil **3**(7): 21-37.
Vandamme, M. and F. J. Ulm (2013). "Nanoindentation investigation of creep properties of calcium silicate hydrates." Cement and Concrete Research **52**: 38-52.
Walraven, J. and A. Bigaj-van Vliet (2013). fib, Model Code for Concrete Structures 2010, Ernst and Son.
Wyrzykowski, M., K. Scrivener and P. Lura (2019). "Basic creep of cement paste at early age-the role of cement hydration." Cement and Concrete Research **116**: 191-201.
Zhang, Q., R. Le Roy, M. Vandamme and B. Zuber (2014). "Long-term creep properties of cementitious materials: Comparing microindentation testing with macroscopic uniaxial compressive testing." Cement and Concrete Research **58**: 89-98.